Biogeosciences

Carbon budget estimation of a subarctic catchment using a dynamic ecosystem model at high spatial resolution

J. Tang[1,2], **P. A. Miller**[1], **A. Persson**[1], **D. Olefeldt**[3], **P. Pilesjö**[1], **M. Heliasz**[1], **M. Jackowicz-Korczynski**[1], **Z. Yang**[4], **B. Smith**[1], **T. V. Callaghan**[5,6,7], **and T. R. Christensen**[1,8]

[1]Department of Physical Geography and Ecosystem Science, Lund University, Sölvegatan 12, 223 62 Lund, Sweden
[2]Department of Resource and Environmental Science, Wuhan University, Road Luoyu 129, Wuhan, China
[3]Department of Renewable Resources, University of Alberta, Edmonton AB T6G 2H1, Canada
[4]Department of Forest Ecosystems and Society, Oregon State University, Corvallis 973 31, Oregon, USA
[5]Royal Swedish Academy of Sciences, Lilla Frescativägen 4A, 114 18 Stockholm, Sweden
[6]Department of Animal and Plant Sciences, University of Sheffield, Sheffield S10 2TN, UK
[7]Department of Botany, National Research Tomsk State University, 36, Lenin Ave., Tomsk 634050, Russia
[8]Arctic Research Centre, Aarhus University, C.F. Møllers Allé 8, 8000 Aarhus C, Denmark

Correspondence to: J. Tang (lu.gistangjing@gmail.com)

Abstract. A large amount of organic carbon is stored in high-latitude soils. A substantial proportion of this carbon stock is vulnerable and may decompose rapidly due to temperature increases that are already greater than the global average. It is therefore crucial to quantify and understand carbon exchange between the atmosphere and subarctic/arctic ecosystems. In this paper, we combine an Arctic-enabled version of the process-based dynamic ecosystem model, LPJ-GUESS (version LPJG-WHyMe-TFM) with comprehensive observations of terrestrial and aquatic carbon fluxes to simulate long-term carbon exchange in a subarctic catchment at 50 m resolution. Integrating the observed carbon fluxes from aquatic systems with the modeled terrestrial carbon fluxes across the whole catchment, we estimate that the area is a carbon sink at present and will become an even stronger carbon sink by 2080, which is mainly a result of a projected densification of birch forest and its encroachment into tundra heath. However, the magnitudes of the modeled sinks are very dependent on future atmospheric CO_2 concentrations. Furthermore, comparisons of global warming potentials between two simulations with and without CO_2 increase since 1960 reveal that the increased methane emission from the peatland could double the warming effects of the whole catchment by 2080 in the absence of CO_2 fertilization of the vegetation. This is the first process-based model study of the temporal evolution of a catchment-level carbon budget at high spatial resolution, including both terrestrial and aquatic carbon. Though this study also highlights some limitations in modeling subarctic ecosystem responses to climate change, such as aquatic system flux dynamics, nutrient limitation, herbivory and other disturbances, and peatland expansion, our study provides one process-based approach to resolve the complexity of carbon cycling in subarctic ecosystems while simultaneously pointing out the key model developments for capturing complex subarctic processes.

1 Introduction

The high latitudes are experiencing greater temperature increases than the global average (AMAP, 2012; IPCC, 2013). Low decomposition rates due to the cold environment have led to an accumulation of large pools of carbon (C) in litter, soils and peatlands, much of which is currently held in permafrost (Tarnocai et al., 2009; Koven et al., 2011; Hartley et al., 2012). However, these C stores may be mineralized rapidly to the atmosphere due to the warming effects on soil microbial activity and thereby increase atmospheric concentrations of both carbon dioxide (CO_2) and methane (CH_4). Meanwhile, temperature-induced vegetation changes

may mitigate those effects by photosynthetic enhancement, which is, however, greatly influenced by disturbances such as plant–herbivore interactions as well as soil water and nutrient contents (Jonasson and Michelsen, 1996; Van Bogaert et al., 2009; Keuper et al., 2012). It is becoming crucial to understand those aspects of vulnerable high-latitude ecosystems and their responses to climate warming (Callaghan et al., 2013). Ecosystems fix atmospheric C through photosynthesis and return this C back through diverse paths and in different forms. In recent years, many field measurements have been carried out in subarctic and arctic environments to quantify C exchanges between the atmosphere and the biosphere. Those measurements enable us to better understand possible feedbacks from terrestrial biota and responses to the changing climate (Bäckstrand et al., 2010; Christensen et al., 2012). However, some concerns about field measurements in the subarctic/arctic environment have been raised and the following research needs have been identified:

1. Complete year-round observations are generally missing, and many studies focus only on growing season measurements (Grogan and Jonasson, 2006; Roulet et al., 2007; Christensen et al., 2012; McGuire et al., 2012). Year-around observations are needed because there is clear evidence that C fluxes in the cold seasons are very important (Larsen et al., 2007b; Mastepanov et al., 2008).

2. Observations of interactions between terrestrial and aquatic systems are lacking (Lundin et al., 2013; Olefeldt et al., 2013). Quantifications of terrestrial lateral loss of C are needed not only because they represent a significant fraction of net ecosystem exchange (NEE) but also because they are intrinsically linked to downstream aquatic C cycling (Lundin et al., 2013). Integrating terrestrial and aquatic C cycling is of high importance for our understanding of the C balance at the catchment scale, particularly at high latitudes. Northern peatlands are large sources of dissolved organic carbon (DOC), while receiving lakes are generally net sources of both CO_2 and CH_4 (Tranvik et al., 2009).

Many environmental characteristics of the Stordalen catchment, located in the subarctic discontinuous permafrost region of northern Sweden, have been measured since the 1950s (Bäckstrand, 2008) and many studies covering a variety of disciplines are still ongoing (Callaghan et al., 2010, 2013). Observations related to the dynamics of almost all the relevant C components have been made in different land-cover types (Christensen et al., 2012; Callaghan et al., 2013). However, the various observations over different land-cover types have not yet been integrated into a comprehensive, year-round catchment-level C budget. A significant aspect of this area is that it contains permafrost that is rapidly thawing (Åkerman and Johansson, 2008). This makes more C hydrologically available (Olefeldt and Roulet, 2012), and the

large stock of C in these tundra soils becomes available to microbial processes (Sjögersten and Wookey, 2002; Fox et al., 2008; Hartley et al., 2012). A rapidly changing environment together with comprehensive observations has established the unique importance of this area as a model system for furthering our process-based understanding of the role of climate changes in northern regions. Furthermore, this understanding, gained in an accessible and highly instrumented area, can be applied to vast areas where large C stocks exist but long-term measurements are lacking.

The Stordalen catchment contains several distinct land-cover types, including tundra heath, birch forest with heath understory, peatlands and lakes/rivers. Hereafter, the peatland is divided into three groups named "palsa", "*Sphagnum* site" and "*Eriophorum* site", based on surface hydrology, permafrost condition and characteristic plant communities. An earlier compilation of the C balance of the larger Torneträsk catchment, which encompasses the Stordalen catchment, indicated that there was a significant sink capacity in the birch forest as well as across the peatland (Christensen et al., 2007). This assessment, however, lacked year-round measurement of CO_2 and CH_4 emissions and did not include direct measurements of aquatic C fluxes (Christensen et al., 2007). Subsequent observations in the Stordalen catchment have focused on filling the missing components. Consequently, recently updated year-round CO_2 and CH_4 measurements in the peatland identified the wetter non-permafrost *Eriophorum* sites to be strong C sinks ($-46\,\mathrm{g\,C\,m^{-2}\,yr^{-1}}$) with high CH_4 emissions (18–22 $\mathrm{g\,C\,m^{-2}\,yr^{-1}}$; Jackowicz-Korczyński et al., 2010; Christensen et al., 2012), while measurements conducted on the drier palsa (where permafrost is present) showed a relatively weaker uptake ($-39.44\,\mathrm{g\,C\,m^{-2}\,yr^{-1}}$; Olefeldt et al., 2012). Total waterborne C exports (DOC plus particulate organic C (POC) and dissolved inorganic C (DIC)) from the terrestrial ecosystems (both peatland and forest) were also monitored (Olefeldt et al., 2013) and found to represent a significant component of the net ecosystem C balance, ranging from 2.77 to 7.31 $\mathrm{g\,C\,m^{-2}\,yr^{-1}}$. In contrast, 4 years of continuous eddy covariance (EC)-tower-based CO_2 measurements in the birch forest revealed very variable C sink/source functionality, which in 2 out of 4 years has been found to be a C source to the atmosphere (Heliasz, 2012). Tundra heath, another important land-cover type in this region, has lower C uptake (Christensen et al., 2007; Fox et al., 2008) and both birch forest and tundra heath were found to have high spatial heterogeneity (Fox et al., 2008; Heliasz, 2012). Altogether, different land-cover types show diverse contributions to this subarctic ecosystem's C balance. With pronounced future warming expected in this region, the structure and function of the different vegetation types are expected to vary dramatically as has been observed during warming in the recent past (Callaghan et al., 2013). In addition, changes to soil conditions due to warming and permafrost thaw will likely stimulate C fluxes to the atmosphere and affect the long-term ac-

cumulated C (Wolf et al., 2008a; McGuire et al., 2012), but this likely C release needs to be weighed against the possibility of increased uptake by increased primary productivity resulting from longer growing seasons and/or potential CO_2 fertilization.

The field measurements described above provide an insight into the ongoing processes and current ecosystem status, but until now, no modeling exercises have been implemented in this region in combination with the comprehensive measured data. Moreover, high-spatial-resolution predictions of future potential dynamics of both vegetation and soil processes and their responses to the projected climate are lacking in this region. In this study, therefore, we aim to assess the Stordalen catchment C budget in a retrospective as well as in a prognostic way by implementing a process-based dynamic ecosystem model (Smith et al., 2001; Miller and Smith, 2012) integrated with a distributed hydrology model (Tang et al., 2014a, b) at high spatial resolution (50 by 50 m; Yang et al., 2012). We quantify the overall C budget of the study catchment by synthesizing diverse C fluxes and specifically address the following questions: (1) will this subarctic catchment become a C source or a larger C sink in the near future? (2) How differently will the catchment's vegetation microtypes respond to the climate drivers? (3) What are the major limitations in the model's prognostic ability?

To answer these questions, we implemented an Arctic-enabled version of the dynamic ecosystem model, LPJ-GUESS WHyMe (Wania et al., 2009a, b, 2010). This model has been widely and successfully implemented for estimating and predicting ecosystem function in high-latitude regions (McGuire et al., 2012; Miller and Smith, 2012; Zhang et al., 2013). LPJ-GUESS WHyMe includes comprehensive process descriptions to capture the interactions between atmosphere–vegetation–soil domains and it explicitly describes permafrost and peatland processes, which are important components of our study catchment. Importantly, previous studies (Tang et al., 2014a, b) dedicated to integrating a distributed hydrology scheme to LPJ-GUESS WHyMe have demonstrated the necessity of considering lateral water movements to accurately capture water and C cycling in this region. The model with distributed hydrology is called LPJG-WHyMe-TFM, where TFM stands for "triangular form-based multiple-flow algorithm" (Pilesjö and Hasan, 2014). The study presented here is the first modeling exercise to combine all the available year-round measured data in the Stordalen catchment and at high spatial resolution.
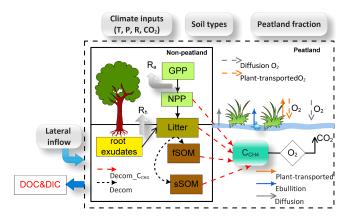
2 Model descriptions

The process-based dynamic ecosystem model LPJG-WHyMe-TFM was chosen as the platform for studying the subarctic catchment C balance. The processes in the model include vegetation growth, establishment and mortality, disturbance, competition between plant individuals for light and soil water (Smith et al., 2001, 2014), and soil biogeochemical processes (Sitch et al., 2003). These processes are operated in a number of independent and replicate patches. Vegetation in the model is defined and grouped by plant function types (PFTs), which are based on plant phenological and physiognomical features combined with bioclimatic limits (Hickler et al., 2004; Wramneby et al., 2008). Bioclimatic conditions determine which PFTs can potentially grow in study regions, and vertical stand structure together with soil water availability further influence PFT establishment based on PFTs' shade and drought tolerance characteristics. A list of the simulated PFTs in this catchment can be found in Table S1 in the Supplement. The parameterization and choice of non-peatland PFTs in this study cover all the main vegetation types found in the study region (boreal forest, shrubs, open-ground grasses) and are based on previous studies for the arctic region using LPJ-GUESS (Wolf et al., 2008a; Hickler et al., 2012; Miller and Smith, 2012; Zhang et al., 2013). For peatland grid cells, two new peatland PFTs, flood-tolerant graminoids and *Sphagnum* moss, are introduced by Wania et al. (2009b).

The model is driven by monthly/annual climate data and includes both non-peatland and peatland hydrological processes (Fig. 1). The vertical water movement between atmosphere, vegetation and soil is based on Gerten et al. (2004), while the lateral water movement between grid cells was implemented by Tang et al. (2014b) based on topographical variations. More recently, an advanced multiple-flow algorithm, TFM (Pilesjö and Hasan, 2014), was chosen to distribute water among grid cells, due to its better treatment of flow continuity and flow estimation over flat surfaces (Tang et al., 2014a). Within the catchment boundary, surface and subsurface runoff can move from one upslope cell to multiple downslope cells, which greatly improves hydrological flux estimations (Tang et al., 2014a) and results in a better estimate of C fluxes in peatland region. The soil temperature estimation is driven by surface air temperature, and the Crank–Nicolson heat diffusion algorithm (Crank and Nicolson, 1996) is implemented to calculate the soil temperature profile on a daily time step (Wania et al., 2009a). The C cycling descriptions in LPJG-WHyMe-TFM for peatland cells are based on Wania's developments (Wania et al., 2009a, b, 2010), while the non-peatland grid cell C cycling is kept the same as in LPJ-GUESS (Smith et al., 2001; Sitch et al., 2003). The full hydrological processes and peatland C cycling descriptions in LPJG-WHyMe-TFM can be found in Sect. S1 in the Supplement. A brief summary of the most relevant C cycling processes in the model will be presented below.

A modified Farquhar photosynthesis scheme (Haxeltine and Prentice, 1996; Haxeltine et al., 1996; Sitch et al., 2003) is used to estimate gross primary production (GPP), which is related to air temperature (T), atmospheric CO_2 concentration, absorbed photosynthetically active radiation (PAR) and stomatal conductance. Part of the GPP is respired to the at-

Figure 1. Schematic of carbon components and cycling in LPJG-WHyMe-TFM. The solid-line box includes carbon cycling for non-peatland cell, whereas the items inside the dashed-line box represent processes particular to the peatland cells. Only DOC&DIC in red text is not explicitly presented in the current model. T: air temperature; P: precipitation; R: radiation; CO_2: atmospheric CO_2 concentration; Decom_C_{CH_4}: decomposed materials allocated to C_{CH_4}; Decom: decomposition.

mosphere by maintenance and growth respiration (R_a), and the remaining part is net primary production (NPP) for each PFT. The reproduction costs are subtracted from NPP, and thereafter the remaining NPP is allocated to different living tissues in accordance with a set of PFT-specific allometric relationships (Smith et al., 2001). Leaves, fine root biomass and root exudates are transferred to the litter pool with a given turnover rate, and above-ground plant materials can also provide inputs to the litter pool due to stochastic natural disturbance events and mortality (Smith et al., 2001; Thonicke et al., 2001). The majority (70 %) of the litter is respired as CO_2 directly to the atmosphere, with a fixed fraction entering into fast- and slow-turnover soil organic pools (fSOM and sSOM; Sitch et al., 2003). The overall decomposition rate in the model is strongly influenced by soil temperature and moisture (Sitch et al., 2003). Additionally, the model also estimates emissions of biogenic volatile organic compounds (BVOC) per PFT (Arneth et al., 2007; Schurgers et al., 2009). However, the modeled BVOC values are not compared in the current study, because they only represent a very small fraction of the modeled NEE and, additionally, there are insufficient growing season measurement data in the study domain to evaluate model performance. The major C cycling pathways can be found in the solid-line box area of Fig. 1. For peatland cells, an extra potential C pool for methanogens (C_{CH_4}) has been added (see dashed-line box area in Fig. 1) and mainly includes root exudates and easily decomposed materials (Wania et al., 2010). The majority of C_{CH_4} is located in the acrotelm layer (Sect. S1) and the oxidation and production of CH_4 together determine the net emission of CH_4. In the model, the oxidation of CH_4 through methanotrophic bacteria is turned into CO_2, whereas the unoxidized

CH_4 can be released to the atmosphere by plant transport, diffusion and ebullition (see the solid-line arrows in Fig. 1). The oxidation level is mainly determined by the location of water table position (WTP) in the model (Wania et al., 2010).

The biomass production in the current version of LPJ-GUESS WHyMe has no representation of nitrogen (N) limitation and neither N fluxes nor C–N interactions are included (Sitch et al., 2007). The latest version of LPJ-GUESS does include N cycling and N limitation on plant production (Smith et al., 2014), but this capability has not yet been integrated with the customized arctic version of the model adopted in the present paper. Moreover, processes determining concentrations of DOC and DIC in soil water have not yet been explicitly described in the model (Fig. 1). To cover the majority of dissolved C losses and gains in our assessment of the catchment C budget, DOC is estimated by combining modeled runoff with observed DOC concentrations. Measured DIC export data are used directly, based on observations by Olefeldt et al. (2013).

3 Study site and materials

3.1 Stordalen catchment

The Stordalen catchment, located in the discontinuous permafrost region, is situated around 9.5 km east of the Abisko Naturvetenskapliga Station (ANS, Abisko Research Station; 68°20′ N, 19°03′ E). The catchment, covering around 16 km², has a steep topography on the southern part and turns into the lower flat peatland region to the north (Fig. 2b). The mean air temperature obtained from ANS records was -0.7 °C for the period 1913–2002 (Christensen et al., 2004) and 0.49 °C for the period 2002–2011 (Callaghan et al., 2013). Climate details of the two warming periods in 20th century are given in Callaghan et al. (2010). The Stordalen catchment is composed of birch forest, tundra heath, peatland, lakes and rivers. Permafrost is only found in the palsa, and recent permafrost loss and conversion of palsa into non-permafrost *Eriophorum* sites have been related to the observed warming trends in the region (Åkerman and Johansson, 2008). The *Sphagnum* sites have a variable active layer depth and are dominated by *Sphagnum* spp. (PFT: pmoss), while the *Eriophorum* sites are dominated by flood-tolerant *Eriophorum* spp. (PFT: WetGRS). Birch forest (PFT: IBS, *Betula pubescens* ssp. *czerepanovii*), which forms the treeline in this region, is mainly distributed around and to the south of the peatlands and extends upwards to mountain slope areas (Fig. 2). Above the birch treeline, there are extensive areas of subarctic ericaceous dwarf-shrub heath dominated by the evergreen species *Vaccinium vitis-idaea* and the deciduous species *V. uliginosum* and *V. myrtillus*. Willow shrubs (*Salix* spp.) and dwarf birch shrubs (*Betula nana*) occur at the fringes of the forest and in wetter areas above treeline. The heath shrub species also occur as a ground layer
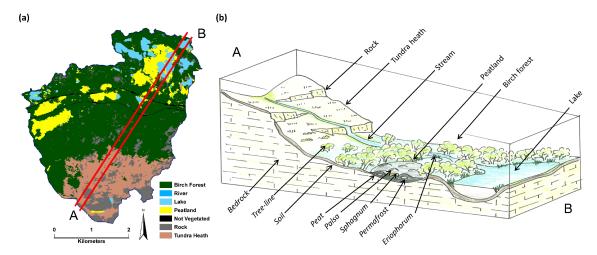
Figure 2. Object-based vegetation classification map of the Stordalen catchment **(a)** and schematic of land-cover types and features of the approximate transect A–B in **(b)**.

in the forest (see Callaghan et al. , 2013, for details of vegetation distribution and changes). Around 5 % of the catchment is covered by lakes or small rivers (Lundin et al., 2013). A detailed description of catchment hydrological conditions can be found in Olefeldt et al. (2013). The map in Fig. 2a is based on an object-based vegetation analysis in this area (Lundin et al., 2015). The classification is based on an aerial imagery data set collected in August 2008, with a spatial resolution of 0.08 by 0.08 m.

3.2 Model inputs and modeling protocol

3.2.1 Model inputs

Monthly climate data at 50 m resolution, including temperature, precipitation and cloudiness, together with annual CO_2 concentration, were used to drive the model from 1913 to 2080 for the Stordalen catchment. The detailed descriptions of data sources for the period of 1913–2010 can be found in Tang et al. (2014b). The high spatial resolution of monthly temperature for the period 1913–2000 was developed by Yang et al. (2011) to cover the whole catchment, while precipitation and cloudiness were extracted and interpolated from the Climatic Research Unit 1.2 data set (Mitchell et al., 2004). For the period 2001–2012, we obtained 12 years of observed temperature and precipitation data from ANS and interpolated these data to the whole region (Olefeldt et al., 2013). The annual CO_2 concentrations from 1913 to 2010 were obtained based on McGuire et al. (2001) and TRENDS (http://cdiac.esd.ornl.gov/trends/co2/contents. htm). The model was spun up in order to achieve vegetation and C pools in equilibrium with the climate at the beginning of the study period by using the first 30 years of climate forcing data to repeatedly drive the model for 300 years. To run the model into the future, the monthly anomalies of simulation outputs from the Rossby Centre Atmosphere-Ocean

(RCAO) regional climate model (Koenigk et al., 2011) for the grid cell nearest Stordalen were estimated and applied to the historical data sets at 50 m, assuming the same anomaly for all cells in the study region. RCAO climate data were downscaled for an arctic domain using boundary forcing from a general circulation model forced by emissions from the SRES A1B scenario for the period 2013–2080 (Zhang et al., 2013).

A soil map provided by the Geological Survey of Sweden was used to identify the peatland fraction of each cell. Notably, the detailed rock area shown in Fig. 2a is not represented by the soil map used. An imagery digital elevation model (DEM) from the National Land Survey of Sweden was used, and the TFM algorithm (written in a MATLAB script, R2012) was used to calculate topographic indices (Pilesjö and Hasan, 2014) used in the model LPJG-WHyMe-TFM.

3.2.2 Additional model parameterization and sensitivity testing

An artificially adjusted snow density ($100\,\mathrm{kg\,m^{-3}}$, following the measurements ranges provided in Judson and Doesken, 2000) was implemented for the birch forest to mimic deeper trapped snow in the forest. The observed thick top organic soil in the birch forest (Heliasz, 2012) is also represented in the model by increasing the organic fraction of the top 0.1 m soil layer (Olefeldt and Roulet, 2014) in the model. Additionally, the model simulation uses a single replicate patch in each 50 m grid cell. Finally, an additional simulation was performed in which we kept the CO_2 concentration constant after 1960 and allowed the remaining inputs to vary as normal to diagnose the extent to which the CO_2 concentration influences on ecosystem dynamics and C fluxes.

3.3 Model evaluation data

The observations used to evaluate the model include (1) EC-tower-measured CO_2 NEE covering the palsa and *Sphagnum* sites during 2008 and 2009 (Olefeldt et al., 2012); (2) EC-tower-measured CO_2 NEE at the *Eriophorum* site from 2006 to 2008 (Christensen et al., 2012); (3) 2 years (2006–2007) of EC-tower-measured CH_4 fluxes at the *Eriophorum* site (Jackowicz-Korczyński et al., 2010); (4) analyzed DOC concentrations at the palsa/*Sphagnum* site and *Eriophorum* site from 2008 (Olefeldt and Roulet, 2012); (5) measured DIC export and DOC concentration at six sampling points from 2007 to 2009 (Olefeldt et al., 2013); (6) EC-tower-measured birch forest CO_2 NEE for four continuous years, 2007–2010 (Heliasz, 2012); and (7) catchment-level annual CO_2 and CH_4 emission from lakes and streams from 2008 to 2011 (Lundin et al., 2013).

3.4 Calculation of the catchment carbon budget

The catchment level C budget was calculated using estimated C fluxes (CF_i; after first accounting for observed DOC or DIC fluxes, where available) weighted by land-cover fractions (f_i in Eq. 1). The symbol i in Eq. (1) represents different land-cover types – in our case, birch forest, peatland (*Sphagnum* and *Eriophorum* sites), tundra heath and lake/river. To identify the temporal variations in C fluxes, the identification of different land cover (except peatland regions) is based on the dominant PFTs for each grid cell during the reference period of 2001–2012. Additionally, the aerial photo-based classification of different peatland types is also used when estimating peatland fluxes as a whole (Olefeldt et al., 2012).

$$C_{all} = \sum_{i=1}^{i=5} CF_i \cdot f_i \tag{1}$$

4 Results

The modeled C fluxes for birch forest, peatland and tundra heath are first compared with the measured data for the period of observation. The seasonality and magnitudes of the fluxes are evaluated and then used to estimate the catchment-level C budget. The modeled long-term C dynamics during the period 1913–2080 are then presented for different land-cover types, and the catchment-level C budget considering all the available C components is also assessed.

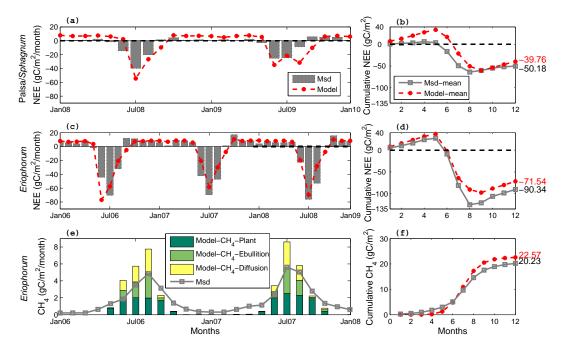## 4.1 Evaluation of the carbon balance in the historical period

4.1.1 Peatland

Both the plant communities and hydrological conditions in the peatland differ among the palsa, *Sphagnum* and *Erio-*

phorum sites. Notably, the measured NEE (see grey bars in Fig. 3a, b) covers both dry hummock (palsa) and semi-wet (*Sphagnum* site) vegetation (Olefeldt et al., 2012), whereas our model cannot represent the dry conditions of the palsa. Therefore, the observed fluxes over both palsa and *Sphagnum* sites were compared with the modeled fluxes at the *Sphagnum* site. The C fluxes magnitudes (including both wintertime emission and summertime uptake) are larger at the *Eriophorum* site when compared with the palsa/*Sphagnum* site for both measured and modeled data. The modeled NEE at both sites generally captures the seasonality and magnitude of measured NEE, from being a strong sink (negative NEE) of CO_2 during the summer (mainly June–August) to being a wintertime CO_2 source. However, the model is unable to fully capture the C source/sink functionality in September at both sites. Furthermore, the modeled winter respiration at the *Eriophorum* site is very close to the observations, though the model overestimates the wintertime emissions at the palsa/*Sphagnum* site. The mean annual cumulative NEE reveals that the model estimations of C fluxes for both parts of the peatland are within the observed ranges, though with around 20 % of underestimation in the 3-year-averaged annual uptake (-39.76 and $-50.18\,\mathrm{g\,C\,m^{-2}\,yr^{-1}}$ for the modeled and observed fluxes at the palsa/*Sphagnum* site; -71.54 and $-90.34\,\mathrm{g\,C\,m^{-2}\,yr^{-1}}$ for the modeled and observed fluxes at the *Eriophorum* site). For the *Eriophorum* site, the 3-year mean growing season uptake of C is underestimated by the model (Fig. 3d), which indicates that the modeled photosynthetic rates may be too low, that summer respiration rates may be too high, or both.

Two full years (2006 and 2007) of EC-tower-measured CH_4 emissions were used to evaluate modeled estimations, and three different pathways of modeled CH_4 are also presented (Fig. 3e, f). The seasonal variability is well described by the model and the modeled cumulative CH_4 over the year shows accurate representation of CH_4 emissions when compared with the observations (20.23 and 22.57 $\mathrm{g\,C\,m^{-2}\,yr^{-1}}$ for the measured and modeled, respectively). Specifically, the wintertime emissions are slightly underestimated, but this underestimation is compensated for by the overestimated summer emissions. Plant-mediated transport of CH_4 dominates during the growing season, while the ebullition and diffusion transport reach a maximum in August. Additionally, the plant-mediated CH_4 emission is the main pathway active during the late spring and early autumn.

4.1.2 Birch forest

The modeled average leaf area index for the birch forest and understory vegetation is around 1.4 and 0.3, respectively, which are consistent with observations made in this area (Heliasz, 2012). Modeled and measured monthly and cumulative NEE are compared for the years 2007–2010 in Fig. 4. From the monthly NEE comparisons (Fig. 4a), we see that the model underestimates ecosystem respired C both before

Figure 3. Monthly (left) and mean annual cumulative (right) CO_2 NEE and CH_4 fluxes for the peatland. Positive values indicate ecosystem release to the atmosphere and negative values indicate ecosystem uptake. Msd stands for measured.
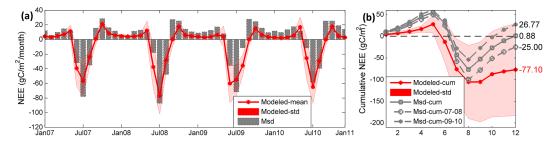
and after the growing season. The maximum photosynthesis-fixed C in July is lower than that measured for the year 2007–2009, but not for the year 2010. The comparisons in Fig. 4b clearly show the cumulative discrepancies between the modeled NEE and the observations. The years 2009 and 2010 become C sources over the year (with the average annual NEE value of $26.77\,\mathrm{g\,C\,m^{-2}\,yr^{-1}}$), even though the measured air temperature for the winter and spring is relatively lower than for the years 2007 and 2008 (mean air temperature for all months apart from June–September is -3.11, -3.56, -4.26 and $-5.75\,°\mathrm{C}$ for the years 2007, 2008, 2009 and 2010, respectively). The abrupt emergence of strong respiration in 2009 and 2010 is not captured by the model. Furthermore, a comparison of the measured and modeled cumulative NEE reveals that the main discrepancy occurs for the winter fluxes. As seen in Fig. 4b, the observed birch forest cumulative CO_2 emissions from January to May reaches $50\,\mathrm{g\,C\,m^{-2}}$, a value which exceeds the range of the model's predictions. Furthermore, the observed CO_2 fluxes in September indicate a C source but the modeled fluxes are close to zero.

The red-shaded areas in Fig. 4a reveal high spatial variations during the growing season and the accumulated variations over the year (the average monthly standard deviations of the 4 years; see Fig. 4b) demonstrate a remarkable spatial variability of the model-estimated annual NEE. Interestingly, the observed mean annual NEE in both 2007–2008 and 2009–2010 fall within the wide spatial variations indicated by the model.

4.1.3 Tundra heath

Around 29.8 % of the catchment with alpine terrain was covered by heaths and dwarf shrubs during the reference period 2001–2012. The model predicts that low-growing evergreen shrubs (PFT: LSE, e.g., *Vaccinium vitis-idaea*) currently dominate in this area, with tall summer-green shrub (PFT: HSS, e.g., *Salix* spp.) dominant in the future predictions (2051–2080; Fig. 5). Since there are no available year-round observations of the C balance in this part of the Stordalen catchment, a synthesis of published data from similar environments is used to evaluate the model estimations (Table 1).

Four periods with averaged C uptake values from our model are presented (see the last four columns in Table 1) and a clear increase in summer uptake can be found with increased temperature and CO_2 concentration. The modeled, whole-year uptake also follows the increasing trend, except for the period of 2051–2080. The model-estimated summer C uptake is much stronger than the observations made at the high-Arctic heath of NE Greenland, which is reasonable when considering the longer growing season in our catchment. The study conducted in an alpine area in Abisko by Fox et al. (2008) shows a wide range of estimated NEE over 40 days during the summertime of 2004. The wide range of NEE values are because three levels of vegetation coverage were studied and the lowest uptake is from sparse vegetation dominated by bare rock and gravels, which is similar to the situation in our tundra heath sites (Fig. 2a). The modeled summer NEE between the years of 2001 and 2012 integrates

Figure 4. Monthly **(a)** and cumulative **(b)** NEE between the years 2007 and 2010 for the birch forest. Modeled NEE with spatial variability (red shadow) for each year is shown.

Table 1. Tundra heath summer and whole year NEE comparisons between the modeled and published data.

Tundra type	Arctic heath	Arctic heath	Arctic heath	Subarctic heath	LSE & HSS	LSE & HSS	LSE & HSS	LSE & HSS
Period	1997, 2000–2005, summer	2007, summer	2007, summer	2004, 13 Jul–21 Aug, 40 days	1961–1990, summer[c]/whole year	1991–2000, summer[c]/whole year	2001–2012, summer[c]/whole year	2051–2080, summer[c]/whole year
Location	NE Greenland	NE Greenland	NE Greenland	Northern Sweden	Northern Sweden	Northern Sweden	Northern Sweden	Northern Sweden
Methods[a]	EC	CH	CH	EC & CH	LPJG	LPJG	LPJG	LPJG
Cumulated NEE	$-1.4 \sim -23.3$[d]	-22.5[e]	-18[e]	$-38.2 \sim -68.7$[f,b]	$-26.89/-4.31$[g]	$-41.83/-12.82$[g]	$-58.23/-31.38$[g]	$-67.93/-26.88$[g]

[a] EC stands for eddy covariance method, CH stands for chamber method and LPJG stands for model estimations with LPJG-WHyMe-TFM. [b] Values vary from sparsely vegetated areas (less than 10 % cover) to fully covered low-growing *Empetrum* areas. [c] The modeled values in summer include data for June, July, August and September. LSE: low-growing (< 50 cm) evergreen shrubs. HSS: tall (< 2 m) deciduous shrubs. [d] Groendahl et al. (2007). [e] Tagesson et al. (2010). [f] Fox et al. (2008). [g] This study.

the whole summer season (longer than 40 days), and falls within the observed ranges presented by Fox et al. (2008), with values slightly higher than the lowest observed values.

4.1.4 Aquatic systems

Lateral waterborne C fluxes

The modeled DOC exports based on runoff estimations are compared with the measured DOC fluxes. The model generally underestimated annual runoff (the measured and modeled mean annual runoff for six points are 279.65 and 207.75 mm, respectively), but the modeled accuracy varies from point to point as well as for different years (Tang et al., 2014a). The average DOC export of the birch forest over 3 years across sampling sites from 2007 to 2009 are 3.65, 2.77 and 2.33 g C m^{-2} yr^{-1} from the observations and 3.09, 2.03 and 1.69 g C m^{-2} yr^{-1} from the model estimations, respectively. The downward trend over the 3 years is captured and is related to lower precipitation during the latter years. The observed DOC export rates at the palsa/*Sphagnum* and *Eriophorum* sites in 2008 are directly used to represent different types of peatland export level and the values are 3.35 and 7.55 g C m^{-2} yr^{-1} for the palsa/*Sphagnum* and *Eriophorum* sites, respectively (Olefeldt and Roulet, 2012). DIC export is currently beyond the scope of our model but nonetheless contributes to the whole C budget. We used an averaged DIC export value of 1.22 g C m^{-2} yr^{-1} based on the published data in Olefeldt et al. (2013) and DIC export is included in the estimation of the catchment C budget below (see Table 2).

Carbon fluxes from lakes and streams

Investigations of aquatic system C emission in the Stordalen catchment were conducted by Lundin et al. (2013) during the years 2008–2011. Around 5 % of the total catchment area (0.75 km^2) is classified as aquatic systems, with lakes accounting for 96 % of the aquatic area. Both lakes and streams contribute to the emissions of CH$_4$ and CO$_2$, but the streams dominate CO$_2$ emission while the lakes dominate CH$_4$ emissions. Averaged across the catchment area, the measured annual CO$_2$ and CH$_4$ emissions from streams are 10.1 and 0.06 g C m^{-2} yr^{-1}, respectively, while the lake emitted 0.5 g C m^{-2} yr^{-1} as CO$_2$ and 0.1 g C m^{-2} yr^{-1} as CH$_4$ (Lundin et al., 2015). Since river and lake processes are at present beyond the scope of the model, the contribution of aquatic systems to the catchment C fluxes is purely based on the observed data (see Table 2).

4.2 Modeled whole-catchment carbon balance

One of the benefits of using a dynamic vegetation model is that it allows us to investigate the vegetation and C-budget responses to climate change. In this section, annual variations of both climate variables (temperature and precipitation) and different ecosystem C fluxes are presented for the whole simulated period. In addition, the normalized catchment C budget is also estimated.

Our simulation results suggest that the temperature increase (around 2 °C; see Fig. 6a–c) together with a CO$_2$ increase to 639 ppm by 2080 could greatly increase the productivity of the birch forest (Figs. 6, 2a–c and 5) as well as peatland CH$_4$ emissions (see Fig. 6a–c). The DOC export

Table 2. Summary of catchment C budget for different time periods. Both mean and annual variations (1-standard-deviation value in the parentheses) of each period are presented. Negative mean values indicate ecosystem carbon uptake, while positive values indicate that mean ecosystem carbon is lost through respiration or CH_4 emission. The mean temperature (T, °C) of each period is listed.

Periods	Birch CO_2[a]	*Eriop.* CO_2[a]	Palsa/*Sphag.* CO_2[a]	Peatland CH_4	Tundra heath	Streams CO_2[c]	Lakes CO_2[c]	Streams CH_4[c]	Lakes CH_4[c]	Birch DIC	Peatland DIC	Birch DOC	*Eriop.* DOC	Palsa/*Sphag.* DOC	C budget
1961–1990 ($T = -1.26$)	−17.52 (22.46)	−36.83 (30.80)	−18.04 (31.39)	14.08 (1.57)	−4.31 (15.81)							2.52 (0.73)			−1.47 (18.25)
2000–2005 ($T = 0.13$)	−3.48 (34.10)	−32.85 (28.91)	−10.49 (27.36)	17.65 (2.21)	−1.63 (21.77)							3.25 (0.56)			7.96 (27.00)
2006–2011 ($T = -0.19$)	−56.68 (44.26)	−60.10 (25.98)	−37.26 (24.58)	18.60 (1.27)	−50.27 (27.28)							2.31 (0.67)			−38.71 (34.55)
2051–2080 ($T = 0.90$)	−24.56 (39.05)	−28.84 (32.25)	−8.43 (27.67)	22.94 (3.71)	−26.88 (32.22)							2.86 (0.40)			−11.23 (33.11)
Measured (years)	0.88[e] (2007–2010)	−90.34[f] (2006–2008)	−50.18[g] (2008–2009)	20.23[f,b] (2006–2007)	−3[d,h]	10.1 ± 4.4[i] (2009–2011)	0.5 ± 0.2[i] (2008–2011)	0.06[i] (2009–2011)	0.1 ± 0.1[i] (2010)	1.22[j] (2007–2009)	1.22[j] (2007–2009)	3.17[j] (2008–2009)	7.55[k] (2008)	3.35[k] (2008)	

[a] Fluxes minus DOC and DIC export. [b] Observed CH_4 fluxes for the *Eriophorum* site. [c] Variables are normalized to the catchment area. [d] Reference-estimated value.
[e] Heliasz (2012). [f] Jackowicz-Korczyński et al. (2010). [g] Olefeldt et al. (2012). [h] Christensen et al. (2007). [i] Lundin et al. (2015). [j] Olefeldt et al. (2013). Eriop.: *Eriophorum*;
[k] Olefeldt and Roulet (2012) *Sphag.*: *Sphagnum*.
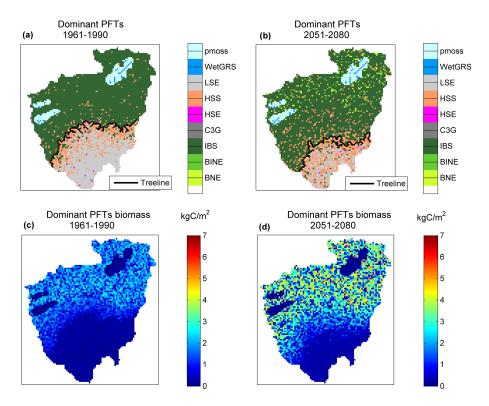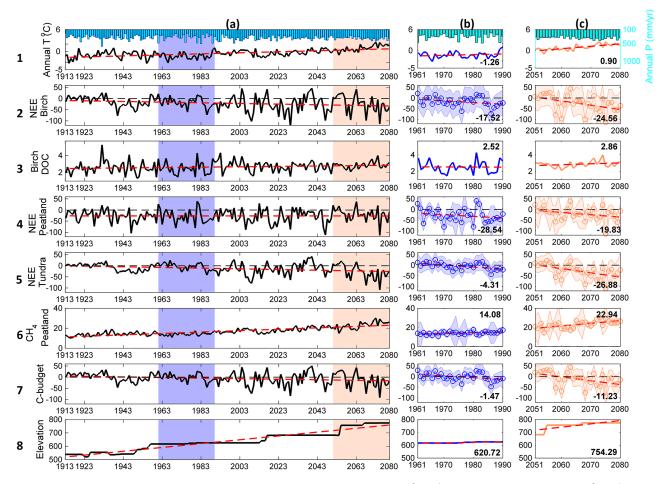

Figure 5. Dominant PFTs **(a, b)** and their biomass **(c, d)** in the study catchment, for the periods 1961–1990 **(a, c)** and 2051–2080 **(b, d)**.

from birch sites also increases slightly over the study period (Fig. 6, 3a–c). Besides leading to an increase in ecosystem biomass in grid cells currently occupied by birch forest (Fig. 5c, d), warming will also result in the current tundra heath close to the birch treeline being replaced by an upward expansion of the birch forest (Fig. 5a, b). This is indicated by the changes to birch treeline's uppermost elevation in Fig. 6, 8a–c. The dramatic increase in C uptake in the tundra heath region (Fig. 6, 5a–c) is largely a result of this vegetation succession. Meanwhile, the successive degradation of permafrost and slightly higher annual precipitation may result in more anaerobic conditions for the modeled peat-

land. Combined with warmer soil conditions, these result in both higher decomposition rates of soil organic matter and greatly increased CH_4 production. Moreover, a stronger response of respiration than NPP to the temperature increase reduces the net C uptake in the peatland (see Fig. 6, 4a–c). The catchment, as a whole, shows an increased C uptake (see the trend line in Fig. 6, 7a) over the 1913–2080 period. The averaged C budgets for the two selected periods (1961–1990 and 2051–2080) are −1.47 and −11.23 g C m^{-2} yr^{-1}, respectively, with the increase being dominated by the large increase seen in the uptake rates at the birch forest and tundra heath sites.

Figure 6. Time series **(a)** of annual mean temperature, precipitation sum, NEE ($g\,C\,m^2\,yr^{-1}$), averaged DOC export ($g\,C\,m^2\,yr^{-1}$) from the birch forest, birch treeline elevation (m) and catchment C budget ($g\,C\,m^2\,yr^{-1}$) values between 1913 and 2080. The NEE data for the birch forest and the peatland have had the corresponding DOC and DIC values subtracted. Here the averaged C fluxes from the Stordalen peatland (the northeast side of the catchment) are used to represent for the averaged C fluxes for the whole-catchment peatlands since only the Stordalen peatland DOC and DIC observations are currently available. The aerial photo-based classification of the *Eriophorum* and Palsa/*Sphagnum* peatland fractions within the Stordalen peatland is used to scale up the C fluxes. The trend of each data set is shown with a red dashed line. The second and third columns **(b, c)** of the figure focus on the periods 1961–1990 and 2051–2080 (these two periods are also indicated in the first column with shaded area). The numbers in bold in columns **(b)** and **(c)** show the annual average of each quantity for the respective time period. The fractions of peatland, birch forest, tundra and lakes/rivers are 5.7, 57.69, 29.76 and 5 %, respectively. Approximately 1.79 % of the catchment area is estimated as being dominated by C3G and HSE, which are not included in the above classification. The last row shows the birch treeline elevation changes over the period.

During the 2051–2080 period, both boreal needleleaf shade-tolerant spruce (PFT: BNE, e.g., *Picea abies*) and boreal needleleaf (but less shade-tolerant) pine (PFT: BINE, e.g., *Pinus sylvestris*) start to appear in the birch-dominated regions (Fig. 5). In the current tundra regions, the coverage of HSS greatly increases at the expense of LSE. For the northern parts of the catchment, birch forest densification is observed with future warming, while the greatest relative changes in biomass occur near the treeline. The increased temperature together with increased CO_2 concentration by 2080 are very likely to increase CO_2 uptake in both tundra heath and forested areas, though the nutrient limitations are not included in this version of the model (but see Smith et al.,

2014). A summary of the modeled catchment C components and C fluxes from different sources is given in Table 2. Additionally, the modeled estimations during the warm period of 2000–2005 are also presented in Table 2, and the positive mean value of catchment C budget is seen to be an exception with reference to the main reference period. Furthermore, the annual variations of the modeled C fluxes in different periods are also presented in Table 2. We find that different land-cover types could shift rapidly from being a C sink to a C source in the future (see the mean plus 1 SD value).

To illustrate the impact of CO_2 increases alone on the modeled C budget, the differences between simulations (ΔC fluxes) with and without a CO_2 increase since 1960 are

shown in Fig. 7. The original outputs of those two simulations are plotted separately in Fig. S1 in the Supplement, together with the statistical significance values (p). Interestingly, the simulation with constant CO_2 forcing after 1960 significantly reduces the birch and tundra uptake (positive values in Fig. 7), whereas the peatland NEE and CH_4 are not strongly influenced by the CO_2 increase. The catchment C-budget dynamics are consistent with the changes seen in the birch and tundra heath regions. Furthermore, the magnitudes of ΔC fluxes for the birch and tundra NEE show an increasing trend after 1971, which is also seen in the ΔC fluxes for the annual GPP and respiration (see birch forest site in Fig. 7a). Since tundra heath shows a similar trend to birch forest, it is not presented in the figure. However, the relative differences of ΔC fluxes for the annual GPP and ecosystem respiration widen over time, which indicates a stronger response of GPP to the increased CO_2 concentration than ecosystem respiration.

To account for the fact that CH_4 is a more potent greenhouse gas than CO_2, an estimation of the global warming potential (GWP) of the two simulations can be made. Assuming the relative climate impact of CH_4 is 28 times greater than CO_2 over a 100-year period (IPCC, 2013), the calculated GWP for the simulation with atmospheric CO_2 increase is 3 times larger in the period 1961–1990 (27.3 g CO_2-eq) than the period 2051–2080 (8.8 g CO_2-eq). However, in the simulation without CO_2 increase, the GWP in 1961–1990 (40.7 g CO_2-eq) is approximately half of the GWP value for the 2051–2080 period (93.3 g CO_2-eq). This shows that the change in global warming potential found in the model simulations is strongly influenced by the CO_2 concentration used to force the model, as the CO_2 trajectory can alter the balance between the GWP changes resulting from C uptake in the birch forest and tundra and the peatland CH_4 emissions.

5 Discussion

To our knowledge, our model simulation is the first attempt to create a C budget of a subarctic catchment based on a dynamic global vegetation model applied at the local scale and to predict its evolution in response to a changing climate. The C-budget estimations in this paper include major flux components (CO_2, CH_4 and hydrological C fluxes) based on a process-based approach. The magnitude and seasonality of modeled C fluxes compare well with the measurements (Figs. 3, 4 and Tables 1 and 2), which gives us confidence in the ability of our model to represent the main processes influencing the C balance in this region. Our hope is that, by using a process-based modeling approach at high spatial resolution, our methodology will be more robust in estimating the C budget in a changing future climate than other budget estimation methods (Christensen et al., 2007; Worrall et al., 2007). In response to a climate warming scenario, our model shows a general increase in the C sink in both birch forest

and tundra heath ecosystems, along with greater CH_4 emissions in the catchment (Fig. 6). Integrated over the catchment, our modeled C budget indicates that the region will be a greater sink of C by 2080, though these estimates are sensitive to the atmospheric CO_2 concentration. Nevertheless, the current model setup and simulations still contain limitations in both the historical estimations and predictions. Below we discuss the model's current performance as well as a few existing limitations, and further propose some potential model developments. Most of the studies referred to below have been conducted specifically in the area near the Stordalen catchment or in other regions with similar environments.

5.1 Modeling carbon fluxes for the historical period

5.1.1 Peatland CO_2 and CH_4 emission

The model estimations in the peatland demonstrated skill in representing the relative differences of CO_2 fluxes between the palsa/*Sphagnum* site and *Eriophorum* site. The current model version cannot represent the very dry conditions of the palsa due to the acrotelm–catotelm soil structure (Wania et al., 2009a); therefore, the overestimated emissions rates of CO_2 (Fig. 3a, b) are expected when using the modeled fluxes from the *Sphagnum* site to compare with the measured data covering both the palsa and *Sphagnum* sites (Larsen et al., 2007a; Bäckstrand et al., 2010). The cold-season respiration at the *Sphagnum* site can account for at least 22 % of the annual CO_2 emissions (Larsen et al., 2007a), which is a further reason for the model overestimations. Moreover, at the *Eriophorum* site, the model slightly underestimated summertime uptake, which was found to be related to modeled summer respiration being higher than dark-chamber-measured respiration, though with high spatial variations (Tang et al., 2014a).

The accurate representations of annual CH_4 emissions at the *Eriophorum* sites reflect the model's improved estimations of both hydrological conditions and dynamic C inputs to the C_{CH_4} pools (Fig. 1). With the inclusion of the distributed hydrology at 50 m resolution (Tang et al., 2014a, b), the lower-lying peatland can receive surface runoff from the upslope regions, and the fact that water can rise to a depth of 10 cm above the surface both creates anaerobic conditions in the model and favors the establishment of flood-tolerant graminoid PFTs such as *Carex* spp., which can transport CH_4 to the atmosphere. Under such anaerobic conditions, decomposition rates are restricted and part of the decomposed C becomes CH_4 (Wania et al., 2010). However, the overestimation of CH_4 emissions during summertime is at least partly likely to be linked to the complexity of modeling the ebullition process (Wania et al., 2010). Based on sensitivity testing shown in Wania et al. (2010), the parameter that controls the CH_4 / CO_2 production ratio under anaerobic conditions can strongly impact the ebullition process, so it is important to determine this parameter more accurately in future stud-
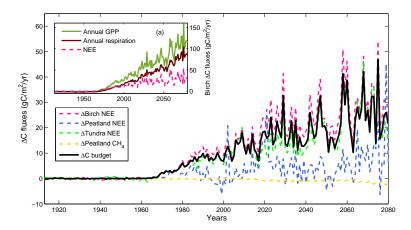
Figure 7. Carbon flux differences (ΔC fluxes) for different land-cover types with and without a CO_2 increase since 1960. Positive values of ΔC NEE imply a higher uptake or a lower emission of CH_4 in the simulations with a CO_2 increase compared to the simulation without a CO_2 increase. For the birch forest land-cover type, the differences in gross primary production (GPP) and ecosystem respiration are shown in the panel **(a)**, where the positive values indicate a higher photosynthesis rate and a higher respiration rate in the simulations with a CO_2 increase compared to the simulations without a CO_2 increase.

ies. Nevertheless, it remains the case that excluding the palsa type could result in a general overestimation of CH_4 emission over the whole peatland.

5.1.2 Wintertime carbon fluxes, thickness of organic layer and disturbance in the birch forest

The high wintertime CO_2 fluxes to the atmosphere observed in the birch forest and the underestimations by our model (Fig. 4) highlight the importance of the representation of winter season C fluxes for the birch forest, particularly as winter temperatures are increasing more than summer temperatures (Callaghan et al., 2010). In the model, the respiration rate is linked to soil temperatures and moisture and the underestimated respiration could be attributed to the lower temperature estimations in the wintertime (covering all months except June–September) when compared with the observed soil temperature at 5 and 10 cm depth in 2009 and 2010 (the modeled wintertime soil temperature is around $1.9\,^\circ\text{C}$ lower than that observed at both depths). Also, the investigations of snow depth insulation influence on soil temperatures and respiratory activity by Grogan and Jonasson (2003) have shown that soil temperature contributes to the greatest variations in respiratory activity at our birch sites. The birch forest is located on the relatively lower parts of the catchment (Fig. 2) and traps the wind-shifted lighter snow from the upland tundra heath, creating a much thicker snow pack and therefore significantly increasing the soil temperatures (Groendahl et al., 2007; Larsen et al., 2007b; Luus et al., 2013). Snow depth measurements in the Abisko birch and tundra heath sites from 24 March to 7 April 2009 (http://www.nabohome.org/cgi-bin/explore.pl?seq=131) revealed that the snowpack in the birch forest was 26.62 cm deeper on average than the snowpack in the tundra heath. The snow density for the birch

forest was artificially decreased to $100\,\text{kg m}^{-3}$ in the model in order to increase the snow depth in the absence of a wind-redistribution mechanism in our model, but it is still hard to capture the high soil temperatures as well as high emission rates in winter.

The thickness of organic soil layer is another crucial component controlling birch site respiration in our catchment (Sjögersten and Wookey, 2002; Heliasz, 2012). The thickness of organic soil is most likely connected to the past transformation of the sites from heath to forest and is expected to decrease if birch biomass continues to increase (Hartley et al., 2012, 2013). Furthermore, Hartley et al. (2012) showed evidence of the decomposition of older soil organic matter during the middle of the growing season and concluded that, with more productive forests in the future, the soil stocks of C will become more labile. From a model perspective, faster turnover rates of soil C pools (Sitch et al., 2007) could be used in climate warming model experiments to reflect the accelerated C mobilization in the soil. This could, to some degree, offset the stronger C uptake in the birch forest site in the simulation results shown here. In addition, the current parameterization of the organic fraction in the birch forest may not fully represent the organic horizons in real-world soil.

The birch forest is cyclically influenced by the outbreak of moths (*E. autumnata*), and an outbreak in 2004 greatly affected the birch forest, resulting in a much lower C uptake than average (Heliasz et al., 2011). Even though it is assumed that the fluxes during 2007–2010 had returned to the pre-defoliation levels (*M. Heliasz*, personal communication, 2013), it is still difficult to completely exclude the influence of insect disturbance in this forest. For the current model simulation, stochastic mortality and patch-destroying disturbance events have been included to account for the impacts of these random processes on ecosystem C cyclings.

However, to give a more accurate and reliable representation of the C fluxes in the birch forest, an explicit representation of insect impacts, outbreaks and their periodicity should be included (Wolf et al., 2008b), as well as other disturbances (Callaghan et al., 2013; Bjerke et al., 2014). For example, a warm event in winter 2007 caused a 26 % reduction in biomass over an area of over $1424 \, \mathrm{km}^2$ in summer 2008 (Bokhorst et al., 2009).

5.1.3 Benefits of high spatial resolution and limitations from monthly temporal resolution

Subarctic ecosystems are characterized by small-scale variations in vegetation composition, hydrological conditions, nutrient characteristics and C fluxes (Lukeno and Billings, 1985; McGuire et al., 2002; Callaghan et al., 2013). The spatial resolution of 50 m in this model application allowed us to capture the diverse vegetation microtypes and their altitudinal gradient in the catchment, as well as their differential responses to climate changes (Figs. 5 and 6). This is unlikely to be well represented by a simple averaging approach across the landscape, e.g., regional or global climate models. Furthermore, it is worth noting that the C cycling in the peatland, especially CH_4 fluxes, is sensitive to the WTP estimations (Tang et al., 2014a). Without spatially distinguished climate and topographical data, it becomes impossible to implement our distributed hydrological scheme and thereby capture the peatland WTP dynamics. To our knowledge, the use of 50 m climate data as forcing of LPJG-WHyMe-TFM (Yang et al., 2011) is among the most detailed and comprehensive modeling exercises related to C cycling. Although this study focuses on C cycling, the innovative projects' changes in vegetation microtypes at high spatial resolution are relevant to local stakeholders such as conservation managers and reindeer herders.

Nevertheless, the high-spatial-resolution data were produced with coarser monthly temporal resolution, which could restrict the model's ability to accurately estimate C fluxes at the start and end of the growing season (Figs. 3 and 4). Due to the dramatic variations of day length at high latitudes, a few days of misrepresenting the starting date of the growing season could significantly alter the estimated plant C uptake (Heliasz, 2012). The daily variations are difficult to capture from the interpolated quasi-daily values used in the model. Indeed, such variations strongly highlight the need for climate forcing at a higher temporal resolution for this region, due to the long daylight duration in summer and short growing seasons.

5.2 Projection uncertainties

A temperature increase of $2\,^\circ\mathrm{C}$ (Fig. 6) and elevated CO_2 concentrations could greatly increase vegetation growth and thus the C sink of the whole catchment. However, the densification and expansion of birch forest as well as the increased presence of boreal spruce and pine PFTs in our projected period (Fig. 5) could be strongly influenced by reindeer grazing and herbivore outbreaks (Hedenås et al., 2011; Callaghan et al., 2013), even though those detected changes are consistent with other models simulations (Wolf et al., 2008a; Miller and Smith, 2012) and general historical trends (Barnekow, 1999). Furthermore, climate warming may favor the spread of insect herbivores, so an assessment of ecosystem responses to future climate change cannot ignore these disturbances (Wolf et al., 2008b) or other factors such as winter warming events (Bjerke et al., 2014).

Temperature increase results in a larger extent of permafrost degradation in the future. Meanwhile, the increased amount of available water from precipitation and lateral inflow may increase the degree of anoxia and further favors the flood-tolerant WetGRS PFT growth as well as CH_4 production. However, the exact extent of wetting or drying of peatland in the future is still highly uncertain, and the model prediction depends strongly on the climate scenario, permafrost thawing, and the resulting balance between increased water availability and increased evapotranspiration. If the peatland drying is large enough, the reduced degree of anoxia could reduce CH_4 emissions in the future (Wrona et al., 2006; Riley et al., 2011). In our case, the peatland, located at the lower part of the catchment, receives water from the southern mountain region, and is more likely to become wetter in the near future in response to the increases in water availability (Wrona et al., 2006). Additionally, the determination of grid cell peat fractions in our simulation is dependent on the current (historical) soil map; therefore, the projections of peatland expansion to non-peatland cells cannot be reflected in the current model predictions. This could bring some additional uncertainties into the catchment C-budget estimations (Malmer et al., 2005; Marushchak et al., 2013).

To cover all the major C components in this catchment, the current estimations of the C budget used available, observed aquatic emissions and DOC concentration and DIC export values, all of which were assumed constant for the whole simulation period, 1913–2080. However, the direction and magnitude of changes to aquatic C fluxes are hard to quantify without modeling additional processes in these systems. Previous studies have found that the substantial thawing of permafrost as well as increased precipitation in recent decades has significantly increased total organic carbon (TOC) concentrations in lakes (Kokfelt et al., 2009; Karlsson et al., 2010). The increased loadings of nutrients and sediments in lakes are very likely to increase productivity of aquatic vegetation, but the effects may be offset by the increased inputs from terrestrial organic C and increases in respiration (Wrona et al., 2006; Karlsson et al., 2010). Emissions of CH_4 from aquatic systems are more likely to increase due to the longer ice-free season (Callaghan et al., 2010), increased methanogenesis in sediments and also increased CH_4 transport by vascular plants (Wrona et al., 2006). Furthermore, a recent study by Wik et al. (2014) found that CH_4 ebullition from

lakes is strongly related to heat fluxes into the lakes. Therefore, future changes to energy fluxes together with lateral transports of dissolved C from terrestrial ecosystems to the aquatic ecosystems are especially important for predicting C emissions from aquatic systems.

As we have discussed, the dynamics of birch forest, and to a lesser extent tundra heath C assimilation, largely determine the catchment's C budget (Figs. 5 and 6), whereas the dramatic increase in CH_4 can slightly offset the net climate impact of the projected C uptake. Furthermore, both modeled C budget and GWP values are very sensitive to the atmospheric CO_2 levels. However, to date, there is no clear evidence showing significant long-term CO_2 fertilization effects in the arctic region (Oechel et al., 1994; Gwynn-Jones et al., 1997; Olsrud et al., 2010). Two possible reasons for this lack of CO_2 fertilization response might be that CO_2 levels close to the moss surface in birch forest can reach as high as 1140 ppm and are normally within the range of 400–450 ppm (Sonesson et al., 1992), while tall vegetation such as shrubs and birch trees as well as peatland species have not been manipulated by CO_2 fertilization. Over the long term, vegetation growth is likely a result of complex interactions between nutrient supplies (McNown and Sullivan, 2013), UV-B exposure (Schipperges and Gehrke, 1996; Johnson et al., 2002), temperature and growing season length (Heath et al., 2005) and forest longevity (Bugmann and Bigler, 2011). Therefore, more field experiments are urgently needed in order to quantify and understand the CO_2 fertilization effects on the various vegetation microtypes of the subarctic environment, and particularly tall vegetation types.

Overall, the current model application has been valuable in pointing to these gaps in process understanding and meanwhile shows the importance of including vegetation dynamics in studies of C balance. Furthermore, a current inability to include the potential impacts of peatland expansion, potential increases of emissions from aquatic systems and the potential nutrient limitations on plants (but see Smith et al., 2014) and disturbances (Bjerke et al., 2014) makes it likely that our projections of the catchment C budget and CO_2 GWP will vary from those that may be observed in the future. However, our high-spatial-resolution, process-based modeling in the subarctic catchment provides an insight into the complexity of responses to climate change of a subarctic ecosystem while simultaneously revealing some key uncertainties that ought to be dealt with in future model development. These developments would be aided by certain new observations and environmental manipulations, particularly of CO_2 with FACE experiments of shrubs and trees, in order to improve our understanding and quantification of complex subarctic processes.

The Supplement related to this article is available online at doi:10.5194/bg-12-2791-2015-supplement.

References

Åkerman, H. J. and Johansson, M.: Thawing permafrost and thicker active layers in sub-arctic Sweden, Permafrost Periglac., 19, 279–292, doi:10.1002/ppp.626, 2008.

AMAP: Arctic Climate Issues 2011: Changes in Arctic Snow, Water, Ice and Permafrost, Oslo, 3 pp., 2012.

Arneth, A., Niinemets, Ü., Pressley, S., Bäck, J., Hari, P., Karl, T., Noe, S., Prentice, I. C., Serça, D., Hickler, T., Wolf, A., and Smith, B.: Process-based estimates of terrestrial ecosystem isoprene emissions: incorporating the effects of a direct CO_2-isoprene interaction, Atmos. Chem. Phys., 7, 31–53, doi:10.5194/acp-7-31-2007, 2007.

Bäckstrand, K.: Carbon gas biogeochemistry of a northern peatland – in a dynamic permafrost landscape, Doctoral, Faculty of Science, Department of Geology and Geochemistry, Stockholm University, 2008.

Bäckstrand, K., Crill, P. M., Jackowicz-Korczyñski, M., Mastepanov, M., Christensen, T. R., and Bastviken, D.: Annual carbon gas budget for a subarctic peatland, Northern Sweden, Biogeosciences, 7, 95–108, doi:10.5194/bg-7-95-2010, 2010.

Barnekow, L.: Holocene tree-line dynamics and inferred climatic changes in the Abisko area, northern Sweden, based on macrofossil and pollen records, The Holocene, 9, 253–265, doi:10.1191/095968399676322637, 1999.

Bjerke, J. W., Stein Rune, K., Kjell Arild, H., Eirik, M., Jane, U. J., Sarah, L., Dagrun, V.-S., and Hans, T.: Record-low primary productivity and high plant damage in the Nordic Arctic Region in 2012 caused by multiple weather events and pest outbreaks, Environ. Res. Lett., 9, 084006, doi:10.1088/1748-9326/9/8/084006, 2014.

Bokhorst, S. F., Bjerke, J. W., Tømmervik, H., Callaghan, T. V., and Phoenix, G. K.: Winter warming events damage sub-Arctic vegetation: consistent evidence from an experimental manipulation and a natural event, J. Ecol., 97, 1408–1415, doi:10.1111/j.1365-2745.2009.01554.x, 2009.

Bugmann, H. and Bigler, C.: Will the CO_2 fertilization effect in forests be offset by reduced tree longevity?, Oecologia, 165, 533–544, doi:10.1007/s00442-010-1837-4, 2011.

Callaghan, T. V., Bergholm, F., Christensen, T. R., Jonasson, C., Kokfelt, U., and Johansson, M.: A new climate era in the sub-Arctic: Accelerating climate changes and multiple impacts, Geophys. Res. Lett., 37, L14705, doi:10.1029/2009GL042064, 2010.

Callaghan, T. V., Jonasson, C., Thierfelder, T., Yang, Z., Hedenås, H., Johansson, M., Molau, U., Van Bogaert, R., Michelsen, A., Olofsson, J., Gwynn-Jones, D., Bokhorst, S., Phoenix, G., Bjerke, J. W., Tømmervik, H., Christensen, T. R., Hanna, E., Koller, E. K., and Sloan, V. L.: Ecosystem change and stability over multiple decades in the Swedish subarctic: complex processes and multiple drivers, Philos. T. R. Soc. B, 368, 20120488, doi:10.1098/rstb.2012.0488, 2013.

Christensen, T. R., Johansson, T., Åkerman, H. J., Mastepanov, M., Malmer, N., Friborg, T., Crill, P., and Svensson, B. H.: Thawing sub-arctic permafrost; effects on vegetation and methane emissions, Geophys. Res. Lett., L04501, 31, 2004.

Christensen, T. R., Johansson, T., Olsrud, M., Strom, L., Lindroth, A., Mastepanov, M., Malmer, N., Friborg, T., Crill, P., and Callaghan, T. V.: A catchment-scale carbon and greenhouse gas budget of a subarctic landscape, Philos. T. Roy. Soc. A, 365, 1643–1656, 2007.

Christensen, T. R., Jackowicz-Korczyński, M., Aurela, M., Crill, P., Heliasz, M., Mastepanov, M., and Friborg, T.: Monitoring the Multi-Year Carbon Balance of a Subarctic Palsa Mire with Micrometeorological Techniques, AMBIO, 41, 207–217, doi:10.1007/s13280-012-0302-5, 2012.

Crank, J. and Nicolson, P.: A practical method for numerical evaluation of solutions of partial differential equations of the heat-conduction type, Adv. Comput. Math., 6, 207–226, doi:10.1007/BF02127704, 1996.

Fox, A. M., Huntley, B., Lloyd, C. R., Williams, M., and Baxter, R.: Net ecosystem exchange over heterogeneous Arctic tundra: Scaling between chamber and eddy covariance measurements, Global Biogeochem. Cy., 22, GB2027, doi:10.1029/2007GB003027, 2008.

Gerten, D., Schaphoff, S., Haberlandt, U., Lucht, W., and Sitch, S.: Terrestrial vegetation and water balance-hydrological evaluation of a dynamic global vegetation model, J. Hydrol., 286, 249–270, doi:10.1016/j.jhydrol.2003.09.029, 2004.

Grogan, P. and Jonasson, S.: Controls on Annual Nitrogen Cycling in the Understory of a Subarctic Birch Forest, Ecology, 84, 202–218, doi:10.1890/0012-9658(2003)084[0202:COANCI]2.0.CO;2, 2003.

Grogan, P. and Jonasson, S.: Ecosystem CO_2 production during winter in a Swedish subarctic region: the relative importance of climate and vegetation type, Glob. Change Biol., 12, 1479–1495, doi:10.1111/j.1365-2486.2006.01184.x, 2006.

Groendahl, L., Friborg, T., and Soegaard, H.: Temperature and snow-melt controls on interannual variability in carbon exchange in the high Arctic, Theor. Appl. Climatol., 88, 111–125, doi:10.1007/s00704-005-0228-y, 2007.

Gwynn-Jones, D., Lee, J. A., and Callaghan, T. V.: Effects of enhanced UV-B radiation and elevated carbon dioxide concentrations on a sub-arctic forest heath ecosystem, Plant Ecol., 128, 243–249, doi:10.1023/A:1009771125992, 1997.

Hartley, I. P., Garnett, M. H., Sommerkorn, M., Hopkins, D. W., Fletcher, B. J., Sloan, V. L., Phoenix, G. K., and Wookey, P. A.: A potential loss of carbon associated with greater plant growth in the European Arctic, Nature Clim. Change, 2, 875–879, doi10.1038/nclimate1575, 2012.

Hartley, I. P., Garnett, M. H., Sommerkorn, M., Hopkins, D. W., and Wookey, P. A.: The age of CO_2 released from soils in contrasting ecosystems during the arctic winter, Soil Biol. Biochem., 63, 1–4, doi:10.1016/j.soilbio.2013.03.011, 2013.

Haxeltine, A. and Prentice, I. C.: BIOME3: An equilibrium terrestrial biosphere model based on ecophysiological constraints, resource availability, and competition among plant functional types, Global Biogeochem. Cy., 10, 693–709, doi:10.1029/96GB02344, 1996.

Haxeltine, A., Prentice, I. C., and Creswell, I. D.: A Coupled Carbon and Water Flux Model to Predict Vegetation Structure, J. Veg. Sci., 7, 651–666, 1996.

Heath, J., Ayres, E., Possell, M., Bardgett, R. D., Black, H. I. J., Grant, H., Ineson, P., and Kerstiens, G.: Rising atmospheric CO_2 reduces sequestration of root-derived soil carbon, Science, 309, 1711–1713, doi:10.1126/science.1110700, 2005.

Hedenås, H., Olsson, H., Jonasson, C., Bergstedt, J., Dahlberg, U., and Callaghan, T.: Changes in Tree Growth, Biomass and Vegetation Over a 13-Year Period in the Swedish Sub-Arctic, AMBIO, 40, 672–682, doi::10.1007/s13280-011-0173-1, 2011.

Heliasz, M., Johansson, T., Lindroth, A., Mölder, M., Mastepanov, M., Friborg, T., Callaghan, T. V., and Christensen, T. R.: Quantification of C uptake in subarctic birch forest after setback by an extreme insect outbreak, Geophys. Res. Lett., 38, L01704, doi:10.1029/2010GL044733, 2011.

Heliasz, M.: Spatial and temporal dynamics of subarctic birch forest carbon exchange, Doctoral, Department of Physical Geography and Ecosystems Science, Lund University Sweden, 132 pp., 2012.

Hickler, T., Smith, B., Sykes, M. T., Davis, M. B., Sugita, S., and Walker, K.: Using a generalized vegetation model to simulate vegetation dynamics in northeastern USA, Ecology, 85, 519–530, doi:10.1890/02-0344, 2004.

Hickler, T., Vohland, K., Feehan, J., Miller, P. A., Smith, B., Costa, L., Giesecke, T., Fronzek, S., Carter, T. R., Cramer, W., Kühn, I., and Sykes, M. T.: Projecting the future distribution of European potential natural vegetation zones with a generalized, tree species-based dynamic vegetation model, Global Ecol. Biogeogr., 21, 50–63, doi:10.1111/j.1466-8238.2010.00613.x, 2012.

IPCC: Climate Change 2013: The Physical Science Basis, NY, USA, chapter 08 and 12, 2013.

Jackowicz-Korczyński, M., Christensen, T. R., Bäckstrand, K., Crill, P., Friborg, T., Mastepanov, M., and Ström, L.: Annual cycle of methane emission from a subarctic peatland, J. Geophys. Res.-Biogeo., 115, G02009, doi:10.1029/2008JG000913, 2010.

Johnson, D., Campbell, C. D., Lee, J. A., Callaghan, T. V., and Gwynn-Jones, D.: Arctic microorganisms respond more to elevated UV-B radiation than CO_2, Nature, 416, 82–83, doi:10.1038/416082a, 2002.

Jonasson, S. and Michelsen, A.: Nutrient Cycling in Subarctic and Arctic Ecosystems, with Special Reference to the Abisko and Torneträsk Region, Ecol. Bull., 45, 45–52, 1996.

Judson, A. and Doesken, N.: Density of Freshly Fallen Snow in the Central Rocky Mountains, B. Am. Meteorol. Soc., 81,

1577–1587, doi:10.1175/1520-0477(2000)081< 1577:DOFFSI> 2.3.CO;2, 2000.

Karlsson, J., Christensen, T. R., Crill, P., Förster, J., Hammarlund, D., Jackowicz-Korczynski, M., Kokfelt, U., Roehm, C., and Rosén, P.: Quantifying the relative importance of lake emissions in the carbon budget of a subarctic catchment, J. Geophys. Res.-Biogeo., 115, G03006, doi:10.1029/2010JG001305, 2010.

Keuper, F., van Bodegom, P. M., Dorrepaal, E., Weedon, J. T., van Hal, J., van Logtestijn, R. S. P., and Aerts, R.: A frozen feast: thawing permafrost increases plant-available nitrogen in subarctic peatlands, Glob. Change Biol., 18, 1998–2007, doi:10.1111/j.1365-2486.2012.02663.x, 2012.

Koenigk, T., Döscher, R., and Nikulin, G.: Arctic future scenario experiments with a coupled regional climate model, Tellus A, 63, 69–86, doi:10.1111/j.1600-0870.2010.00474.x, 2011.

Kokfelt, U., Rosen, P., Schoning, K., Christensen, T. R., FÖRster, J., Karlsson, J., Reuss, N., Rundgren, M., Callaghan, T. V., Jonasson, C., and Hammarlund, D.: Ecosystem responses to increased precipitation and permafrost decay in subarctic Sweden inferred from peat and lake sediments, Glob. Change Biol., 15, 1652–1663, doi:10.1111/j.1365-2486.2009.01880.x, 2009.

Koven, C. D., Ringeval, B., Friedlingstein, P., Ciais, P., Cadule, P., Khvorostyanov, D., Krinner, G., and Tarnocai, C.: Permafrost carbon-climate feedbacks accelerate global warming, P. Natl. Acad. Sci., 108, 14769–14774, doi:10.1073/pnas.1103910108, 2011.

Larsen, K. S., Grogan, P., Jonasson, S., and Michelsen, A.: Respiration and Microbial Dynamics in Two Subarctic Ecosystems during Winter and Spring Thaw: Effects of Increased Snow Depth, Arct. Antarct. Alp. Res., 39, 268–276, doi:10.1657/1523-0430(2007)39[268:RAMDIT]2.0.CO;2, 2007a.

Larsen, K. S., Ibrom, A., Jonasson, S., Michelsen, A., and Beier, C.: Significance of cold-season respiration and photosynthesis in a subarctic heath ecosystem in Northern Sweden, Glob. Change Biol., 13, 1498–1508, doi:10.1111/j.1365-2486.2007.01370.x, 2007b.

Lukeno, J. O. and Billings, W. D.: The influence of microtopographic heterogeneity on carbon dioxide efflux from a subarctic bog, Ecography, 8, 306–312, doi:10.1111/j.1600-0587.1985.tb01183.x, 1985.

Lundin, E. J., Giesler, R., Persson, A., Thompson, M. S., and Karlsson, J.: Integrating carbon emissions from lakes and streams in a subarctic catchment, J. Geophys. Res.-Biogeo., 118, 1200–1207, doi:10.1002/jgrg.20092, 2013.

Lundin, E. J., Christensen, T. R., Giesler, R., Heliasz, M., Klaminder, J., Persson, A., and Karlsson, J.: A weak C sink at high latitudes: support from an integrated terrestrial-aquatic C balance, submitted, 2015.

Luus, K. A., Lin, J. C., Kelly, R. E. J., and Duguay, C. R.: Subnivean Arctic and sub-Arctic net ecosystem exchange (NEE): Towards representing snow season processes in models of NEE using cryospheric remote sensing, Prog. Phys. Geogr., 37, 484–515, doi:10.1177/0309133313491130, 2013.

Malmer, N., Johansson, T., Olsrud, M., and Christensen, T. R.: Vegetation, climatic changes and net carbon sequestration in a North-Scandinavian subarctic mire over 30 years, Glob. Change Biol., 11, 1895–1909, doi:10.1111/j.1365-2486.2005.01042.x, 2005.

Marushchak, M. E., Kiepe, I., Biasi, C., Elsakov, V., Friborg, T., Johansson, T., Soegaard, H., Virtanen, T., and Martikainen, P.

J.: Carbon dioxide balance of subarctic tundra from plot to regional scales, Biogeosciences, 10, 437–452, doi:10.5194/bg-10-437-2013, 2013.

Mastepanov, M., Sigsgaard, C., Dlugokencky, E. J., Houweling, S., Strom, L., Tamstorf, M. P., and Christensen, T. R.: Large tundra methane burst during onset of freezing, Nature, 456, 628–630, doi:10.1038/nature07464, 2008.

McGuire, A. D., Sitch, S., Clein, J. S., Dargaville, R., Esser, G., Foley, J., Heimann, M., Joos, F., Kaplan, J., Kicklighter, D. W., Meier, R. A., Melillo, J. M., Moore, B., Prentice, I. C., Ramankutty, N., Reichenau, T., Schloss, A., Tian, H., Williams, L. J., and Wittenberg, U.: Carbon balance of the terrestrial biosphere in the Twentieth Century: Analyses of CO_2, climate and land use effects with four process-based ecosystem models, Global Biogeochem. Cy., 15, 183–206, doi:10.1029/2000GB001298, 2001.

McGuire, A. D., Wirth, C., Apps, M., Beringer, J., Clein, J., Epstein, H., Kicklighter, D. W., Bhatti, J., Chapin, F. S., de Groot, B., Efremov, D., Eugster, W., Fukuda, M., Gower, T., Hinzman, L., Huntley, B., Jia, G. J., Kasischke, E., Melillo, J., Romanovsky, V., Shvidenko, A., Vaganov, E., and Walker, D.: Environmental variation, vegetation distribution, carbon dynamics and water/energy exchange at high latitudes, J. Veg. Sci., 13, 301–314, doi:10.1111/j.1654-1103.2002.tb02055.x, 2002.

McGuire, A. D., Christensen, T. R., Hayes, D., Heroult, A., Euskirchen, E., Kimball, J. S., Koven, C., Lafleur, P., Miller, P. A., Oechel, W., Peylin, P., Williams, M., and Yi, Y.: An assessment of the carbon balance of Arctic tundra: comparisons among observations, process models, and atmospheric inversions, Biogeosciences, 9, 3185–3204, doi:10.5194/bg-9-3185-2012, 2012.

McNown, R. W. and Sullivan, P. F.: Low photosynthesis of treeline white spruce is associated with limited soil nitrogen availability in the Western Brooks Range, Alaska, Funct. Ecol., 27, 672–683, doi:10.1111/1365-2435.12082, 2013.

Miller, P. A. and Smith, B.: Modelling Tundra Vegetation Response to Recent Arctic Warming, AMBIO, 41, 281–291, doi:10.1007/s13280-012-0306-1, 2012.

Mitchell, T. D., Carter, T. R., Jones, P. D., Hulme, M., and New, M.: A comprehensive set of high-resolution grids of monthly climate for Europe and the globe: the observed record (1901–2000) and 16 scenarios (2001–2100), Tyndall Centre, UEA, Norwich, UK, 1–25, 2004.

Oechel, W. C., Cowles, S., Grulke, N., Hastings, S. J., Lawrence, B., Prudhomme, T., Riechers, G., Strain, B., Tissue, D., and Vourlitis, G.: Transient nature of CO_2 fertilization in Arctic tundra, Nature, 371, 500–503, 1994.

Olefeldt, D. and Roulet, N. T.: Effects of permafrost and hydrology on the composition and transport of dissolved organic carbon in a subarctic peatland complex, J. Geophys. Res.-Biogeo., 117, G01005, doi:10.1029/2011jg001819, 2012.

Olefeldt, D. and Roulet, N. T.: Permafrost conditions in peatlands regulate magnitude, timing, and chemical composition of catchment dissolved organic carbon export, Glob. Change Biol., 20, 3122–3136, doi:10.1111/gcb.12607, 2014.

Olefeldt, D., Roulet, N. T., Bergeron, O., Crill, P., Bäckstrand, K., and Christensen, T. R.: Net carbon accumulation of a high-latitude permafrost palsa mire similar to permafrost-free peatlands, Geophys. Res. Lett., 39, L03501, doi:10.1029/2011GL050355, 2012.

Olefeldt, D., Roulet, N., Giesler, R., and Persson, A.: Total waterborne carbon export and DOC composition from ten nested subarctic peatland catchments-importance of peatland cover, groundwater influence, and inter-annual variability of precipitation patterns, Hydrol. Process., 27, 2280–2294, doi:10.1002/hyp.9358, 2013.

Olsrud, M., Carlsson, B. Å., Svensson, B. M., Michelsen, A., and Melillo, J. M.: Responses of fungal root colonization, plant cover and leaf nutrients to long-term exposure to elevated atmospheric CO_2 and warming in a subarctic birch forest understory, Glob. Change Biol., 16, 1820–1829, doi:10.1111/j.1365-2486.2009.02079.x, 2010.

Pilesjö, P. and Hasan, A.: A Triangular Form-based Multiple Flow Algorithm to Estimate Overland Flow Distribution and Accumulation on a Digital Elevation Model, Transactions in GIS, 18, 108–124, doi:10.1111/tgis.12015, 2014.

Riley, W. J., Subin, Z. M., Lawrence, D. M., Swenson, S. C., Torn, M. S., Meng, L., Mahowald, N. M., and Hess, P.: Barriers to predicting changes in global terrestrial methane fluxes: analyses using CLM4Me, a methane biogeochemistry model integrated in CESM, Biogeosciences, 8, 1925–1953, doi:10.5194/bg-8-1925-2011, 2011.

Roulet, N. T., Lafleur, P. M., Richard, P. J. H., Moore, T. R., Humphreys, E. R., and Bubier, J.: Contemporary carbon balance and late Holocene carbon accumulation in a northern peatland, Glob. Change Biol., 13, 397–411, doi:10.1111/j.1365-2486.2006.01292.x, 2007.

Schipperges, B. and Gehrke, C.: Photosynthetic Characteristics of Subarctic Mosses and Lichens, Ecol. Bull., 121–126, 1996.

Schurgers, G., Arneth, A., Holzinger, R., and Goldstein, A. H.: Process-based modelling of biogenic monoterpene emissions combining production and release from storage, Atmos. Chem. Phys., 9, 3409–3423, doi:10.5194/acp-9-3409-2009, 2009.

Sitch, S., Smith, B., Prentice, I. C., Arneth, A., Bondeau, A., Cramer, W., Kaplan, J. O., Levis, S., Lucht, W., Sykes, M. T., Thonicke, K., and Venevsky, S.: Evaluation of ecosystem dynamics, plant geography and terrestrial carbon cycling in the LPJ dynamic global vegetation model, Glob. Change Biol., 9, 161–185, doi:10.1046/j.1365-2486.2003.00569.x, 2003.

Sitch, S., McGuire, A. D., Kimball, J., Gedney, N., Gamon, J., Engstrom, R., Wolf, A., Zhuang, Q., Clein, J., and McDonald, K. C.: Assessing the carbon balance of circumpolar Arctic tundra unsing remoste sensing and process modeling, Ecol. Appl., 17, 213–234, doi:10.1890/1051-0761(2007)017[0213:ATCBOC]2.0.CO;2, 2007.

Sjögersten, S. and Wookey, P. A.: Climatic and resource quality controls on soil respiration across a forest-tundra ecotone in Swedish Lapland, Soil Biol. Biochem., 34, 1633–1646, doi:10.1016/S0038-0717(02)00147-5, 2002.

Smith, B., Prentice, I. C., and Sykes, M. T.: Representation of vegetation dynamics in the modelling of terrestrial ecosystems: comparing two contrasting approaches within European climate space, Global Ecol. Biogeogr., 10, 621–637, doi:10.1046/j.1466-822X.2001.t01-1-00256.x, 2001.

Smith, B., Wårlind, D., Arneth, A., Hickler, T., Leadley, P., Siltberg, J., and Zaehle, S.: Implications of incorporating N cycling and N limitations on primary production in an individual-based dynamic vegetation model, Biogeosciences, 11, 2027–2054, doi:10.5194/bg-11-2027-2014, 2014.

Sonesson, M., Gehrke, C., and Tjus, M.: CO_2 environment, microclimate and photosynthetic characteristics of the moss Hylocomium splendens in a subarctic habitat, Oecologia, 92, 23–29, doi:10.1007/BF00317258, 1992.

Tagesson, T., Mastepanov, M., Tamstorf, M. P., Eklundh, L., Schubert, P., Ekberg, A., Sigsgaard, C., Christensen, T. R., and Ström, L.: Satellites reveal an increase in gross primary production in a greenlandic high arctic fen 1992–2008, Biogeosciences Discuss., 7, 1101–1129, doi:10.5194/bgd-7-1101-2010, 2010.

Tang, J., Miller, P. A., Crill, P. M., Olin, S., and Pilesjö, P.: Investigating the influence of two different flow routing algorithms on soil-water-vegetation interactions using the dynamic ecosystem model LPJ-GUESS, Ecohydrology, doi:10.1002/eco.1526, 2014a.

Tang, J., Pilesjö, P., Miller, P. A., Persson, A., Yang, Z., Hanna, E., and Callaghan, T. V.: Incorporating topographic indices into dynamic ecosystem modelling using LPJ-GUESS, Ecohydrology, 7, 1147–1162, doi:10.1002/eco.1446, 2014b.

Tarnocai, C., Canadell, J. G., Schuur, E. A. G., Kuhry, P., Mazhitova, G., and Zimov, S.: Soil organic carbon pools in the northern circumpolar permafrost region, Global Biogeochem. Cy., 23, GB2023, doi:10.1029/2008GB003327, 2009.

Thonicke, K., Venevsky, S., Sitch, S., and Cramer, W.: The role of fire disturbance for global vegetation dynamics: coupling fire into a Dynamic Global Vegetation Model, Global Ecol. Biogeogr., 10, 661–677, doi:10.1046/j.1466-822X.2001.00175.x, 2001.

Tranvik, L. J., Downing, J. A., Cotner, J. B., Loiselle, S. A., Striegl, R. G., Ballatore, T. J., Dillon, P., Finlay, K., Fortino, K., Knoll, L. B., Kortelainen, P. L., Kutser, T., Larsen, S., Laurion, I., Leech, D. M., Leigh McCallister, S., McKnight, D. M., Melack, J. M., Overholt, E., Porter, J. A., Prairie, Y., Renwick, W. H., Roland, F., Sherman, B. S., Schindler, D. W., Sobek, S., Tremblay, A., Vanni, M. J., Verschoor, A. M., Von Wachenfeldt, E., and Weyhenmeyer, G. A.: Lakes and reservoirs as regulators of carbon cycling and climate, Limnol. Oceanogr., 54, 2298–2314, 2009.

Van Bogaert, R., Jonasson, C., De Dapper, M., and Callaghan, T. V.: Competitive interaction between aspen and birch moderated by invertebrate and vertebrate herbivores and climate warming, Plant Ecol. & Diversity, 2, 221–232, doi:10.1080/17550870903487456, 2009.

Wania, R., Ross, I., and Prentice, I. C.: Integrating peatlands and permafrost into a dynamic global vegetation model; 1, Evaluation and sensitivity of physical land surface processes, Global Biogeochem. Cy., 23, GB3014, doi:10.1029/2008gb003412, 2009a.

Wania, R., Ross, I., and Prentice, I. C.: Integrating peatlands and permafrost into a dynamic global vegetation model; 2, Evaluation and sensitivity of vegetation and carbon cycle processes, Global Biogeochem. Cy., 23, GB3015, doi:10.1029/2008gb003413, 2009b.

Wania, R., Ross, I., and Prentice, I. C.: Implementation and evaluation of a new methane model within a dynamic global vegetation model: LPJ-WHyMe v1.3.1, Geosci. Model Dev., 3, 565–584, doi:10.5194/gmd-3-565-2010, 2010.

Wik, M., Thornton, B. F., Bastviken, D., MacIntyre, S., Varner, R. K., and Crill, P. M.: Energy input is primary controller of methane bubbling in subarctic lakes, Geophys. Res. Lett., 41, 550–560, doi:10.1002/2013GL058510, 2014.

Wolf, A., Callaghan, T., and Larson, K.: Future changes in vegetation and ecosystem function of the Barents Region, Climatic Change, 87, 51–73, doi:10.1007/s10584-007-9342-4, 2008a.

Wolf, A., Kozlov, M., and Callaghan, T.: Impact of non-outbreak insect damage on vegetation in northern Europe will be greater than expected during a changing climate, Climatic Change, 87, 91–106, doi:10.1007/s10584-007-9340-6, 2008b.

Worrall, F., Burt, T., Adamson, J., Reed, M., Warburton, J., Armstrong, A., and Evans, M.: Predicting the future carbon budget of an upland peat catchment, Climatic Change, 85, 139–158, doi:10.1007/s10584-007-9300-1, 2007.

Wramneby, A., Smith, B., Zaehle, S., and Sykes, M. T.: Parameter uncertainties in the modelling of vegetation dynamics-Effects on tree community structure and ecosystem functioning in European forest biomes, Ecol. Modell., 216, 277–290, doi:10.1016/j.ecolmodel.2008.04.013, 2008.

Wrona, F. J., Prowse, T. D., Reist, J. D., Hobbie, J. E., Lévesque, L. M. J., and Vincent, W. F.: Climate Change Effects on Aquatic Biota, Ecosystem Structure and Function, AMBIO, 35, 359–369, doi:10.1579/0044-7447(2006)35[359:CCEOAB]2.0.CO;2, 2006.

Yang, Z., Hanna, E., and Callaghan, T. V.: Modelling surface-air-temperature variation over complex terrain around Abisko, Swedish Lapland: uncertainty of measurements and models at different scales, Geogr. Ann. A, 93, 89–112, doi:10.1111/j.1468-0459.2011.00005.x, 2011.

Yang, Z., Sykes, M., Hanna, E., and Callaghan, T.: Linking Fine-Scale Sub-Arctic Vegetation Distribution in Complex Topography with Surface-Air-Temperature Modelled at 50-m Resolution, AMBIO, 41, 292–302, doi:10.1007/s13280-012-0307-0, 2012.

Zhang, W., Miller, P. A., Smith, B., Wania, R., Koenigk, T., and Döscher, R.: Tundra shrubification and tree-line advance amplify arctic climate warming: results from an individual-based dynamic vegetation model, Environ. Res. Lett., 8, 034023, doi:10.1088/1748-9326/8/3/034023, 2013.